Noise from a Circulation Control Wing with Upper Surface Blowing

M. Salikuddin,* W. H. Brown,† and K. K. Ahuja‡
Lockheed-Georgia Company, Marietta, Georgia

The work presented in this paper represents a first step in understanding and evaluating the noise characteristics of a circulation control wing (CCW) with upper surface blowing (USB). It was found that high frequency noise was dominated by the effects of the circulation control jet and that low frequency noise was dominated by the effects of the upper surface blowing. The individual effects of the CCW and USB can be superimposed to yield a good approximation of the resultant effect in a combined CCW/USB configuration.

Introduction

THE circulation control wing (CCW) concept is a mechanically simple, high lift system that employs tangential blowing over a rounded trailing edge with an expenditure of minimum amounts of jet momentum and mass flow, to yield very high lift augmentation.[1,2] The basic aerodynamics of the circulation control wing concept involve the adherence of a thin, tangentially ejected jet sheet to the rounded trailing edge of an otherwise conventional airfoil. This phenomenon, called the Coanda effect, is produced by a balance within the jet sheet between centrifugal force and the low static pressure lifting force, generated by the jet velocity V_S (Fig. 1a). This device initially provides a blowing-type boundary-layer control, but achieves its high-lift capability by controlling the airfoil stagnation points to increase the circulation around the wing. Due to the absence of a long mechanical flap, this circulation control is achieved at considerably lower momentum coefficients than those needed in the somewhat similar tangentially blown flap systems.[3-5] The primary mechanism of the CCW lift augmentation is the increased streamline deflection, which accompanies movement of the stagnation points; the overall result is to produce an effective camber which is considerably greater than the geometric value.

Further, by combining the circulation control (CC) and with upper surface blowing (USB) in a CCW/USB configuration, as shown in Fig. 1b, some very significant benefits are obtained from the ability of circulation control phenomenon to entrain and control the engine thrust direction.[6,7] The rather complex and heavy USB mechanical flap system and its supporting structure and actuators can be eliminated and replaced by the stationary circulation control (CC) round trailing edge and internal blowing plenum. For the CCW/USB system, the thrust deflection angle depends on the CC plenum pressure, slot mass flow, and the geometry of the CC trailing edge. The CCW thrust deflection angle is changed nearly instantly by a control valve or pressure regulator which modulates the slot mass flow. The thrust can be deflected pneumatically up to 160 deg, thereby providing high lift, the possibility of vertical flight, and thrust reversal, all without complex mechanisms. The near-instantaneous thrust deflection variation provides quick-responding direct lift and flight path control.[8]

All the high-lift benefits of the CCW/USB configuration notwithstanding, the acoustic performance of the configuration is not available in the open literature. Therefore, a CCW/USB model with full-span circulation control ability was designed, fabricated, and tested in Lockheed's free-jet anechoic wind tunnel to evaluate the acoustic performance of this system. The noise measurements were taken in two planes: flyover and sideline. The acoustic performance of the D-shaped nozzle (used for the USB) operated alone, the CCW operated alone, and the USB systems were also evaluated. A limited number of wake survey tests using a five-hole probe to evaluate the thrust-turning capability of the system were also conducted. These results are presented in detail in three Lockheed engineering reports.[9-11] The noise of a circulation control wing with upper surface blowing and forward speed is too complex to permit a thorough analysis in a journal article. Nor was it possible within the scope of the experimental effort to address all the possible interactions of the many variables that are involved. Salient features of noise data from the flyover plane and some wake survey results are presented in a form that makes these results most easily usable by researchers who want to generate noise prediction capabilities.

Experimental Setup and Test Procedure

Measurements to evaluate the acoustic performance of the CCW/USB system and its individual components were carried out in an anechoic free-jet wind tunnel. The facility is capable of providing continuous free-jet velocities up to 105 m/s, with a circular test section of 0.71 m diam.[12]

The USB/CCW model design represents a four-engine aircraft, which can achieve good STOL performance and not be severely penalized in cruise by concessions to high-lift performance.[13] Model and operating variables are summarized in Table 1.

The upper surface blowing was achieved by using a D-shaped nozzle, with the straight edge flush with the wing surface, impinging at an angle of 20 deg to the surface. This impingement angle provides adequate flow spreading over the wing surface. The wing is constructed with a solid leading edge section which is followed by a replaceable trailing-edge section. The replaceable downstream section consists of a set of ribs, top and bottom cover plates, and the circular trailing edge.

The circulation control blowing air was discharged parallel to the Coanda surface and essentially parallel to the flow across the full 48-in. span of the wing's upper surface. This was accomplished by contouring the trailing edge of the adjustable cover plate. The contour was shaped such that the path of the blowing air forms a convergent nozzle. This extra care was required because, at model scale, a straight-cut trail-

Received Dec. 6, 1985; revision received Aug. 28, 1986.

*Scientist Associate. Member AIAA.
†Scientist.
‡Senior Scientist. Member AIAA.

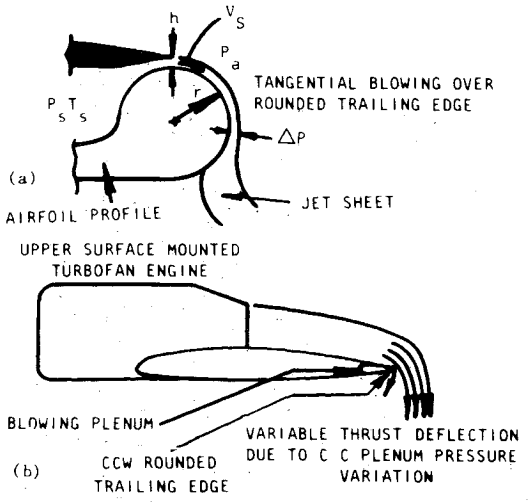

Fig. 1 Powered-lift system emplying CCW combined with USB: a) Basic circulation control aerodynamics. b) CCW/USB engine thrust deflector.

Table 1 CCW/USB model and operating variables

USB nozzle (*D* shape)	
Exit area	4.69 in.^{2} (30.25 cm^2)
Equivalent diameter, d_E	2.44 in. (6.2 cm)
Impingement angle	20 deg
Chordwise position on wing	7.5 in. (19.05 cm)
Wing (symmetrical)	
Chord, *c*	15 in. (38.1 cm)
Thickness, *t*	2.25 in. (5.7 cm)
Trailing edge radius, *r*	0.328 in. (0.83 cm)
Slot height, *h*	0.012–0.048 in. (0.0305–0.122 cm)
Operational variables	
Jet velocity, V_J	0–740 fps (0–225 m/s)
Tunnel velocity, V_T	0–350 fps (0–105 m/s)
Slot velocity, V_S	0–1120 fps (0–340 m/s)
Angle of attack	0 deg

ing edge (which is blunt) forms a convergent-divergent nozzle, or discharges the blowing air at an angle that promotes separation from the Coanda surface.

The experimental configuration is shown in Fig. 2. The D-shaped nozzle was connected to the 10-cm-diam supply duct, at an angle of 20 deg to the axis. The nozzle exit was flush mounted on the midchord and midspan position of the CC wing. A wooden fairing, built for this test configuration, sealed the gap between the nozzle and the leading edge of the wing to minimize interference. The wing was mounted on one anechoic chamber wall, with zero angle of attack, and was placed in front of the 71-cm-diam free-jet nozzle. The midsection of the wing was placed along the vertical central plane of the free-jet nozzle. To accommodate the 20 deg impingement angle of the nozzle and to keep the deflected flow (due to the circulation control) within the bounds of the tunnel flow, the nozzle supply duct was raised in the free-jet 20 cm from the center line. In this position, approximately 58 cm of the wing was immersed in the tunnel flow.

Far field data were measured by several 0.635-cm-diam B&K microphones on a polar arc in the flyover plane. Microphone distances were radially measured from the trailing edge of the wing at the midspan point. Polar angles, θ, were measured from the downstream direction of a line parallel to the tunnel axis and passing through the trailing edge at midspan. Microphones were positioned at 10 deg intervals between $\theta = 40$ and 120 deg. Most of the microphones were at

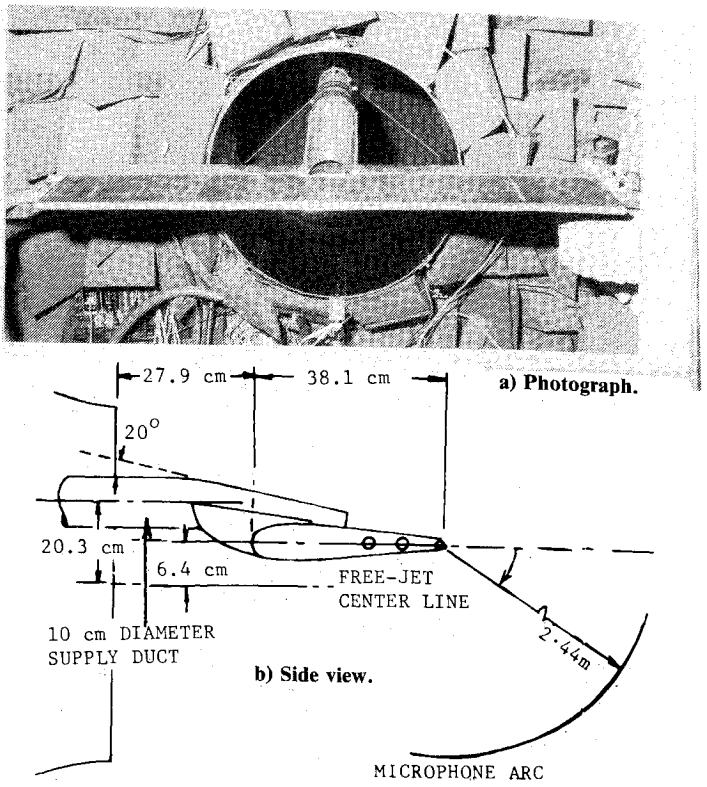

Fig. 2 CCW/USB system installed in the free-jet anechoic wind tunnel.

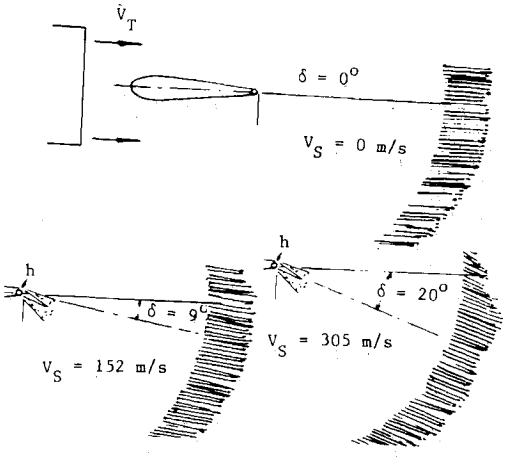

Fig. 3 A typical set of wake survey showing the effect of slot velocity, V_S on the wake velocity profile and the flow deflection angle δ for the CCW-alone configuration; $V_T = 63$ m/s, $h = 1.22$ mm.

a distance of 10 ft (2.44 m) from the midspan trailing edge point. Only a few extreme microphones were placed closer to the trailing edge to avoid interference by the anechoic chamber walls at those angles.

The basic test procedure consisted of measuring the far-field signals with 9 microphones placed on the arc for each test condition. The microphone signals were recorded on a multichannel analog tape recorder for post processing. Reduction to ⅓-octave band spectra was done by using a FFT analyzer followed by processing on a computer to include calibration and tunnel corrections. Apart from the acoustic runs, some wake survey runs were made to examine the relationship between the noise and the thrust deflection angle. A rake of seven five-hole probes was manually traversed in the midspan plane of the wing, at a distance of 1.5 chord lengths (i.e., 57.15 cm) from the trailing edge.

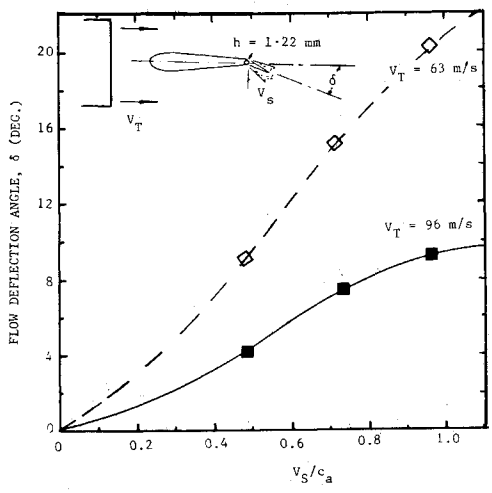

Fig. 4 Effect of slot velocity V_S on the flow deflection angle δ for the CCW-alone configuration, at different flight velocities, V_T.

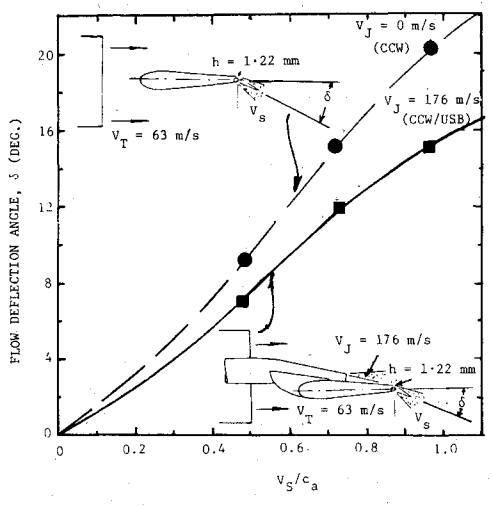

Fig. 5 Effect of slot velocity V_S on the flow deflection angle δ with and without jet velocity V_J; $V_T = 63$ m/s.

Thrust Deflection for the CCW/USB Configuration

A limited number of tests were conducted using a rake of seven five-hole probes to evaluate the thrust-turning capability of the CCW/USB system. The trailing-edge wake survey tests were conducted for the CCW configuration alone, as well as for the CCW/USB combination, to indicate the effect of CC slot blowing on the flow deflection. Noise is the primary thrust of this paper. However, some flow deflection data are presented to help correlate the acoustic performance of the CCW/USB system with its aerodynamic behavior. The boundary layer thickness on the wing was not measured because it is not a major factor in determining the noise of the CCW/USB configuration.

The processing of the measured data involved the conversion of the measured pressures into the resultant velocity vectors. For each position, seven velocity vectors (one for each probe) were generated, covering about 8.9 angular degrees, each being separated by 1.27 deg. Therefore, a continuous wake survey was achieved by moving the probe rake in intervals of 10 deg. The wake velocity vectors thus obtained are plotted on an arc, which is in the midspan plane and centered on the trailing edge. An overall turning angle δ for each flow condition was determined by measuring the vector inclination at several positions.

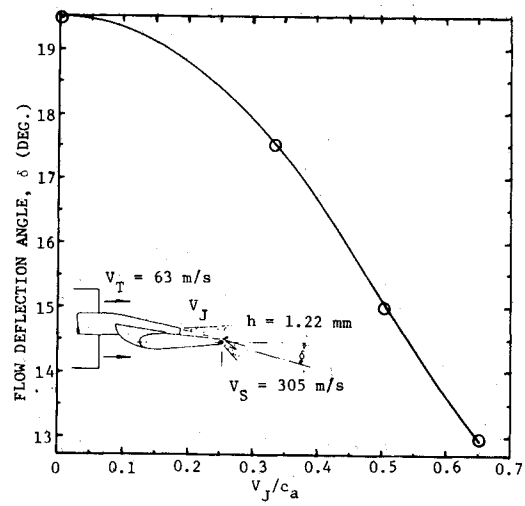

Fig. 6 Effect of jet velocity V_J on the flow deflection angle δ for the CCW/USB configuration; $V_S = 305$ m/s; $V_T = 63$ m/s.

The acoustic characteristics of the CCW/USB system are presented as functions of various flow velocities, which is the usual convention for acoustic data because it is most useful. To correlate the thrust deflection behavior of the CCW/USB configuration with the noise data, the flow turning angles are also presented as functions of various flow velocities (or Mach numbers) instead of the corresponding momentum fluxes. However, other variables have been included in the text so that momentum fluxes, which are directly related to the flow velocities, can be easily computed by the user.

Effect of Slot Velocity

A typical set of wake profiles for the CCW-alone configuration with $V_T = 63$ m/s at different CC jet velocities V_S are plotted in Fig. 3. For $V_S = 0$ m/s, there is no flow turning ($\delta = 0$ deg) and the wake profile is symmetric about the line parallel to the tunnel axis and passing through the chord of the wing. However, with the initiation of the CC jet, the wake flow turns downward. The turning angle δ increases with increasing V_S, and hence with the CC jet momentum. These results are summarized in Fig. 4, where the flow deflection angle δ is plotted with respect to CC Mach number (V_S/c_a) for two different flight velocities. The angle δ increases with increasing V_S (or momentum) for a given V_T. However, the effect of increasing V_T is to reduce the amount of turning angle δ for a fixed V_S. This is due to increased momentum of the freestream.

The effect of the CC jet on the wake profile of the CCW/USB configuration is shown in Fig. 5. In this case, the USB velocity was fixed at $V_J = 176$ m/s, which is equivalent to a fixed thrust level. For $V_S = 0$ m/s, there is no measurable flow turning. However, as soon as the CC jet is turned on, the flow starts turning down and, similar to the CCW-alone configuration, the turning angle δ increases with V_S. As expected, the turning angle δ reduces with increasing V_J. This behavior is also shown in Ref. 13 for the static condition where flow turning angles are plotted with respect to the CC jet momentum for various fixed USB jet momentum levels (i.e., thrusts). In Fig. 5, the variation of δ with V_S for CCW configuration is compared with those for CCW/USB configurations, which includes the D-nozzle and the fairing. It is possible that the deflection angles for CCW/USB configuration could be effected by the D-nozzle and the fairing wakes in the tunnel flow. However, it is reasonable to assume that the influence of these wakes is negligible since the tunnel velocities V_T utilized in the experiments were smaller than the USB (V_J) and CCW jet (V_S) velocities.

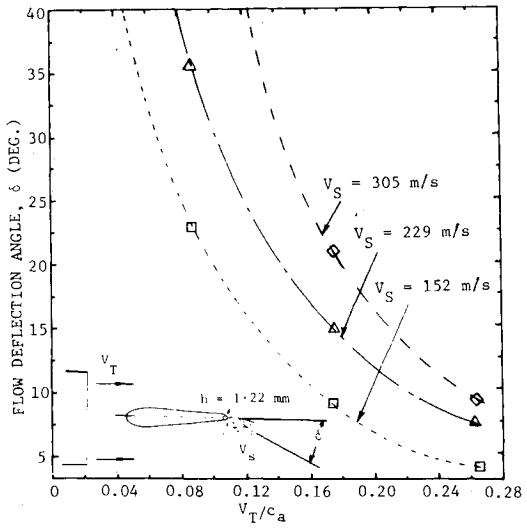

Fig. 7 Effect of flight velocity V_T on the flow deflection angle δ for the CCW-alone configuration at various slot velocities, V_S.

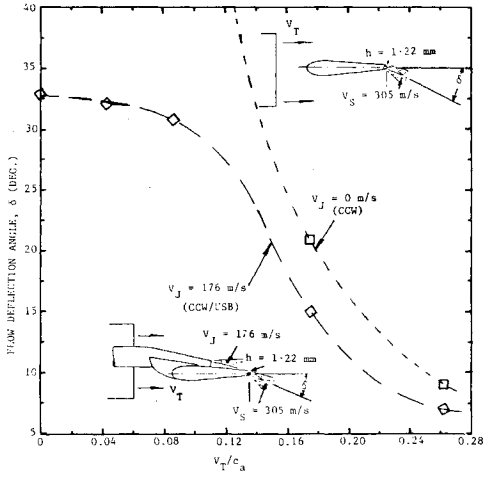

Fig. 8 Velocity of flight velocity V_T on the flow deflection angle δ with and without jet velocity V_J; $V_S = 305$ m/s.

Effect of Upper Surface Blowing

Figure 6 shows the decreasing flow turning angle with increasing V_J for the CCW/USB configuration at various USB flow rates (i.e., thrust levels) and at fixed V_T and V_S. The resultant velocity in the wake increases with increasing V_J. This effect for the static condition is consistent with that shown in Englar et al.[13] and Eppel et al.[14]

Effect of Flight Velocity

Figure 7 shows the effect of flight velocity V_T on flow turning angle at various CC jet velocities V_S. It can be clearly observed that the flow turning angles decrease with increasing V_T and are very high at lower flight velocities. However, the flow turning angle is rapidly decreased with increasing flight speed. The magnitude of the flow turning angle is increased with V_S for a fixed V_T.

The variations of flow turning angle δ with respect to V_T/c_a for the CCW/USB configuration are plotted in Fig. 8, with and without V_J. In the absence of V_J, the flow turning angle is very high at lower flight velocities. For the static condition, as demonstrated in Ref. 14, the flow turning angle is as high as 160 deg. However, as the USB jet is turned on, the flow turning angle drops considerably, even in the static condition, as observed in Fig. 8.

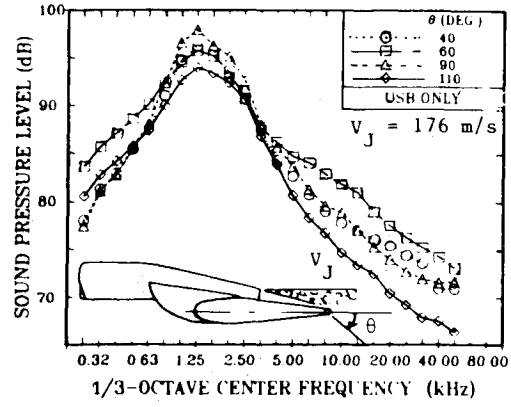

Fig. 9 Spectral variation with polar angle θ; $V_J = 176$ m/s; $V_T = 0$ m/s.

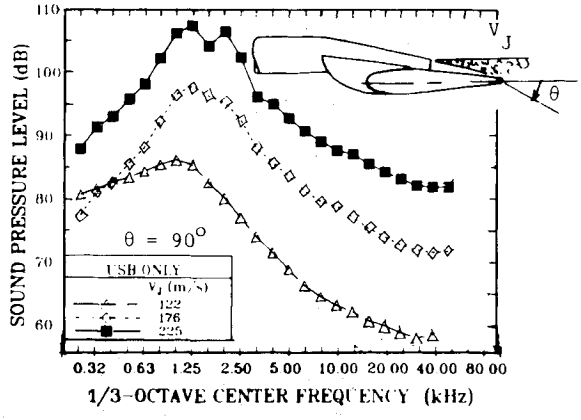

Fig. 10 Increasing SPL's with increasing jet velocity V_J; $\theta = 90$ deg; $V_T = 0$ m/s.

Conclusion

1) The CCW/USB system is able to pneumatically produce thrust deflection similar to that of the lower thrust levels by USB with mechanical flaps.

2) The thrust deflection, or the flow turning angle, increases with increasing CC jet momentum. However, the flow turning angle decreases with a fixed CC jet momentum, with increasing USB and/or increasing flight velocity.

3) The effect of slot height on flow deflection is negligible for a fixed CC jet momentum.[13]

The aerodynamic results presented in this section are very useful in understanding and correlating some of the acoustic behavior of the CCW/USB configuration presented in the following sections of this paper.

Acoustics of the Upper Surface Blowing System

USB configuration was identical to the CCW/USB configuration, except that the slot of the circulation control wing was closed (i.e., $h = 0$) and the air supply to the wing plenum was shut off.

Spectra

Typical ⅓-octave SPL spectra at various polar angles at a given jet velocity are shown in Fig. 9. Clearly, an SPL peak is observed at all polar angles. The peak level and frequency in the spectra increase with increasing jet velocity (not shown

here).[9] These results show that, similar to jet noise of a single nozzle, the effect of increasing flow velocity is to widen the difference between the SPL at small angles and larger angles with the jet axis. This is very clear for the polar angles: 60, 90, and 110 deg.

Jet Velocity Dependence

To examine the effect of increasing velocity on USB noise, the SPL's are plotted for different jet velocities at two polar angles $\theta = 90$ deg in Fig. 10. Based on the results presented in Fig. 10 and in Ref. 9, the sound pressure levels increase at all frequencies and at all polar angles with increasing jet velocities similar to a round nozzle configuration.

To determine a scaling law for the SPL spectra with respect to USB jet velocities (V_J), the Over All Sound Pressure Levels (OASPL's) and the peak SPL's at $\theta = 90$ deg are expressed as $\text{Log}_{10}(V_J/c_a)^m$. The exponent m for OASPL and peak SPL is found to be 7.4 and 7.9, respectively.[9] It should be noted that the similar exponent for a round jet is 8.0.

Acoustics of the Circulation Control Wing

Spectra

Typical ⅓-octave SPL spectra at various polar angles at a given slot velocity are shown in Fig. 11. A low frequency hump (around 2 kHz) is observed at all polar angles. However, this hump tends to merge into the rising broadband noise with increasing slot velocity (not shown here). At this stage, it is not clear what causes this hump. One possible cause is the internal noise generated in the circulation control flow supply duct by the control valve and other hardware.

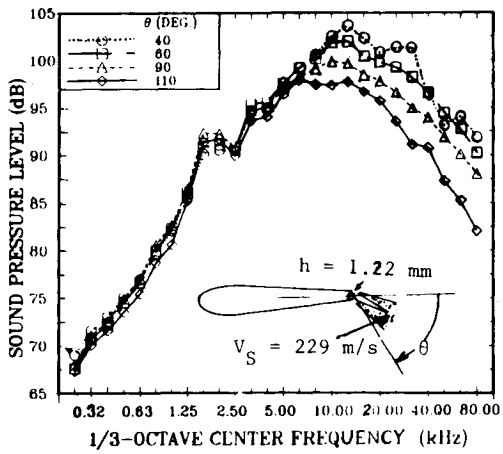

Fig. 11 Spectral variation with polar angle θ; $V_S = 229$ m/s; $V_T = 0$ m/s; $h = 1.22$ mm.

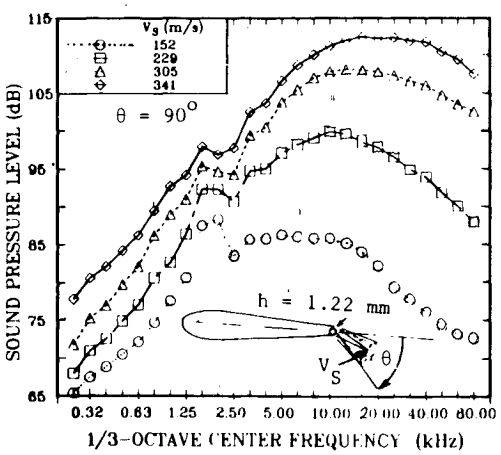

Fig. 12 Increasing SPL's with slot velocity V_S; $\theta = 90$ deg; $V_T = 0$ m/s; $h = 1.22$ mm.

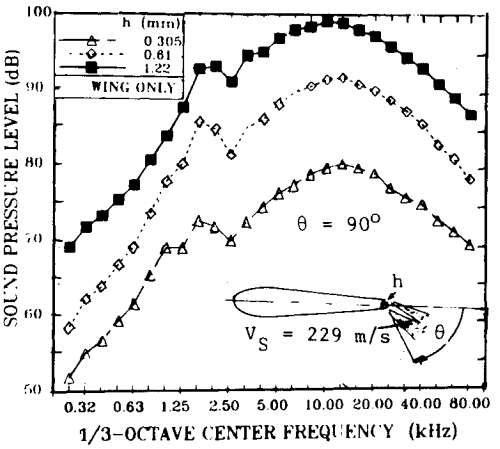

Fig. 13 Increasing SPL's with slot height h; $\theta = 90$ deg; $V_S = 229$ m/s; $V_T = 0$ m/s.

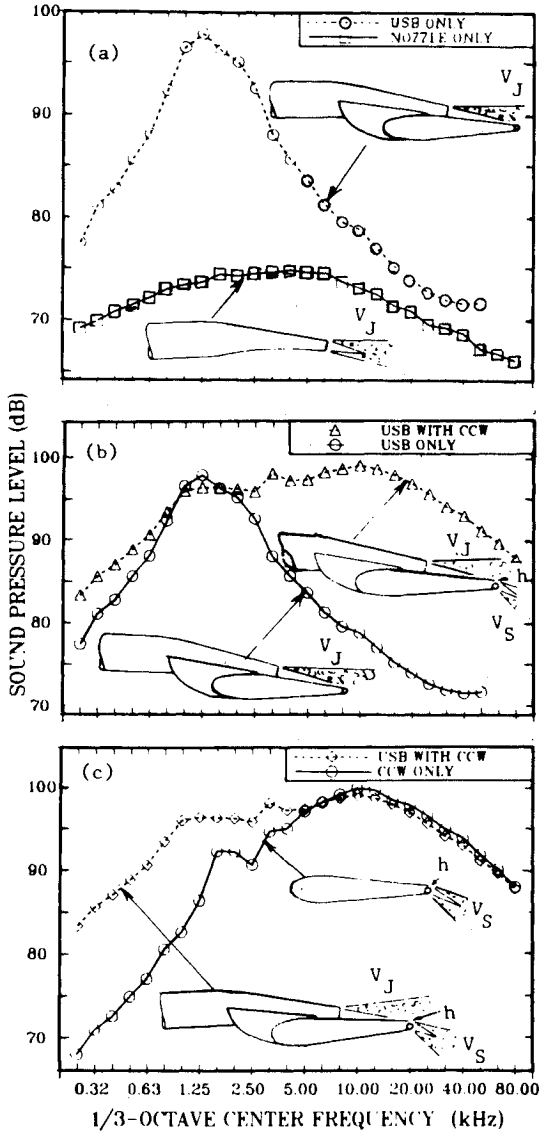

Fig. 14 Comparison of SPL spectra generated by various components of the CCW/USB system; $V_T = 0.0$ m/s; $V_J = 176$ m/s; $V_S = 229$ m/s; $h = 1.22$ mm; and $\theta = 90$ deg.

Other than this hump, an additional peak in the spectra is observed at all polar angles and slot velocities.[9] The levels and the frequencies of this peak increase with increasing slot velocity. Unlike the jet noise of a single nozzle, the effect of increasing slot velocity is to reduce the difference between the SPL at small angles and larger angles with the jet axis, but only at high frequencies.

Slot Velocity Dependence

To examine the effect of increasing slot velocity on the CCW noise, the SPL's are plotted for different slot velocities at $\theta = 90$ deg in Fig. 12. As observed in Fig. 12 and Ref. 9, the sound pressure levels at all frequencies and the frequency at the peak SPL increase with increasing slot velocity for all polar angles. A scaling law, similar to that for the USB jet, was also applied to the CCW jet velocity V_S. The exponent m for OASPL and peak SPL at $\theta = 90$ deg and $h = 1.22$ mm is found to be 7.35 and 7.5, respectively.[9] The exponents for other angles (θ) and for other slot heights (h) could be different; they were not investigated in this study.

Slot Height Dependence

To examine the effect of slot height on the CCW noise for a fixed slot velocity of 229 m/s, the SPL's are plotted for different slot heights at $\theta = 90$ deg in Fig. 13. As observed in Fig. 13 and Ref. 9, the sound pressure levels increase at all frequencies and at all polar angles with increasing slot velocity, which is qualitatively similar to a round jet. However, the shift of SPL peak frequency with respect to slot height is small compared to that for a corresponding change in the diameter of a round jet. The increase in peak SPL at $\theta = 90$ deg due to the change in slot height from 0.305 to 1.22 mm (4 times), is about 18 dB, which does not quantitatively follow the round jet behavior for exit area scaling.

Acoustic Characteristics of a CCW with USB

In this section, the acoustic behavior of the interaction of CC with USB is described. To appreciate the acoustic behavior of the CCW/USB system, it is worthwhile to summarize the effects of individual components and their interactions for a typical condition.

Figure 14 shows typical SPL spectra for various CCW/USB components at $\theta = 90$ deg with jet velocity $V_J = 176$ m/s (upper surface blowing) and slot velocity $V_S = 229$ m/s for the static condition. The salient results are as follows.

Figure 14a: The effect of upper surface blowing is to produce levels of as much as 25 dB higher than the D-nozzle alone. As described in Ref. 9, the increased noise due to upper surface blowing is believed to be generated by the interaction between the disturbances in the free shear layer of the wall jet and the trailing edge of the wing.

Figure 14b: On adding CCW to the USB configuration, additional high frequency noise of as much as 30 dB more than that produced by the USB-alone configuration is generated. The noise generated by a round jet with an equivalent exit area is much lower than that of the CCW jet. This indicates that a slot jet with very high aspect ratio (i.e., 1000) certainly behaves in a different manner than a round jet. The core region in this case is very small compared to that of an equivalent round jet. In addition, the lower side of the slot jet is attached to the rounded surface of the trailing edge, which makes it a wall jet on a curved wall. All of these are possible contributors to the higher observed noise levels.

Figure 14c: All of the high frequency augmentation is generated by the CCW blowing, whereas the low frequency noise is mostly contributed by the USB.

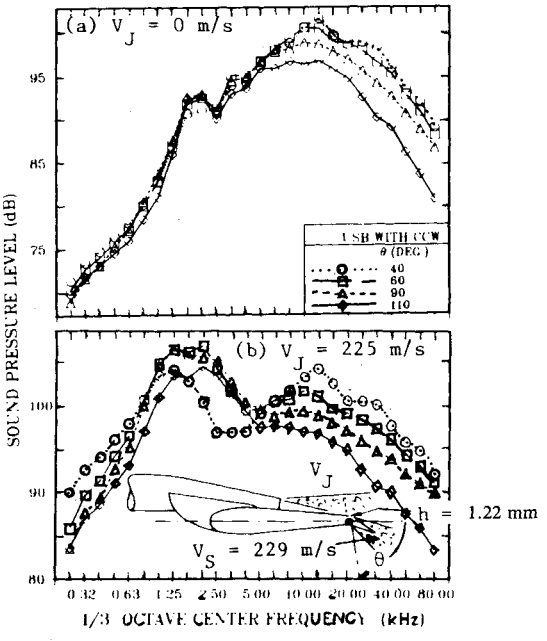

Fig. 15 Spectral variation with polar angle θ without and with jet velocity V_J; $V_T = 0$ m/s; $V_S = 229$ m/s; $h = 1.22$ mm.

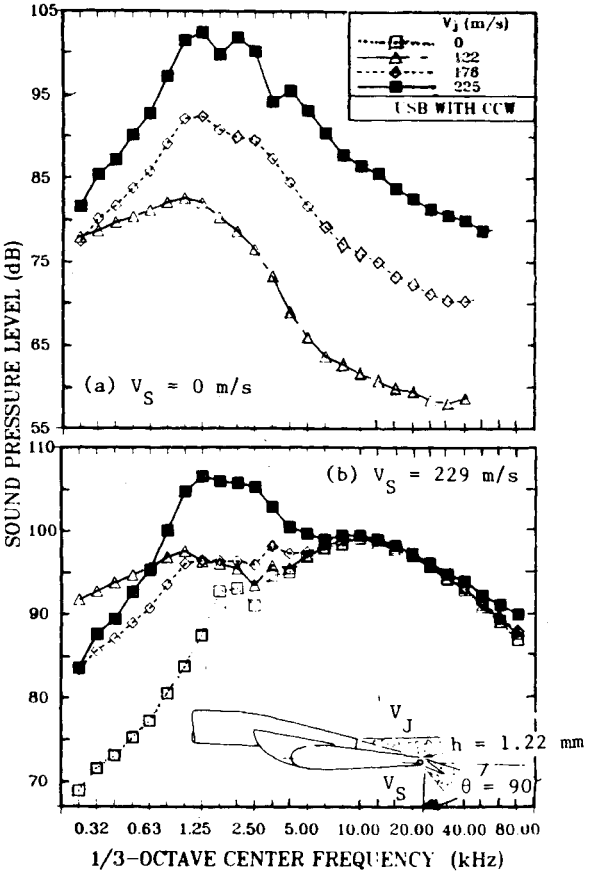

Fig. 16 Spectral variation with jet velocity V_J at two slot velocities V_S; $\theta = 90$ deg; $V_T = 0$ m/s; $h = 1.22$ mm.

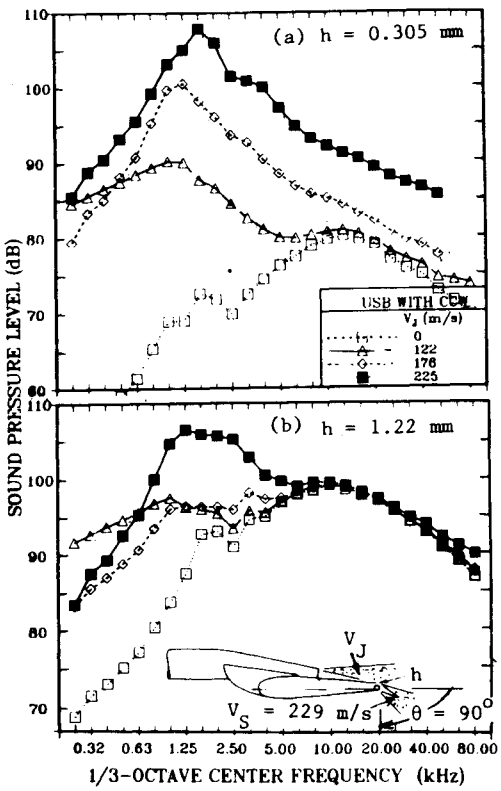

Fig. 17 Spectral variation with jet velocity V_J at two slot heights h; $\theta = 90$ deg; $V_T = 0$ m/s; $V_S = 229$ m/s.

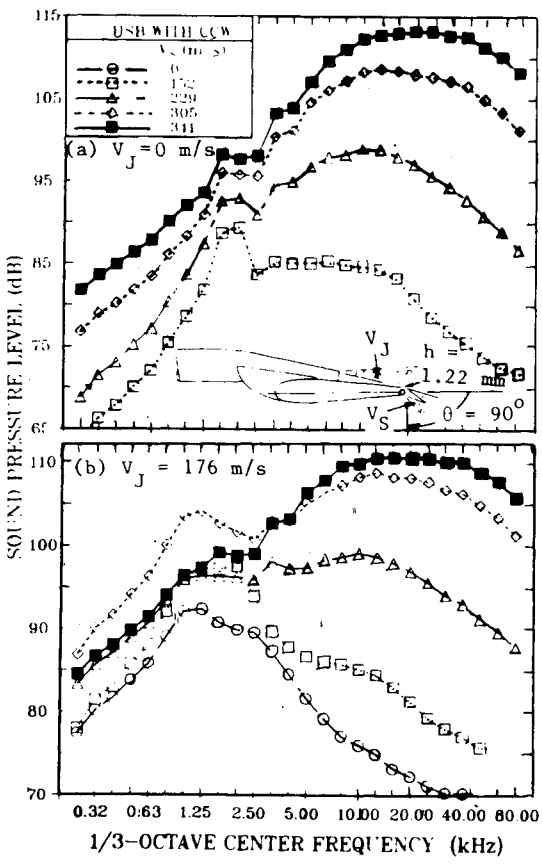

Fig. 18 Increasing SPL's with slot velocities V_S at two jet velocities V_J; $\theta = 90$ deg; $V_T = 0$ m/s; $h = 1.22$ mm.

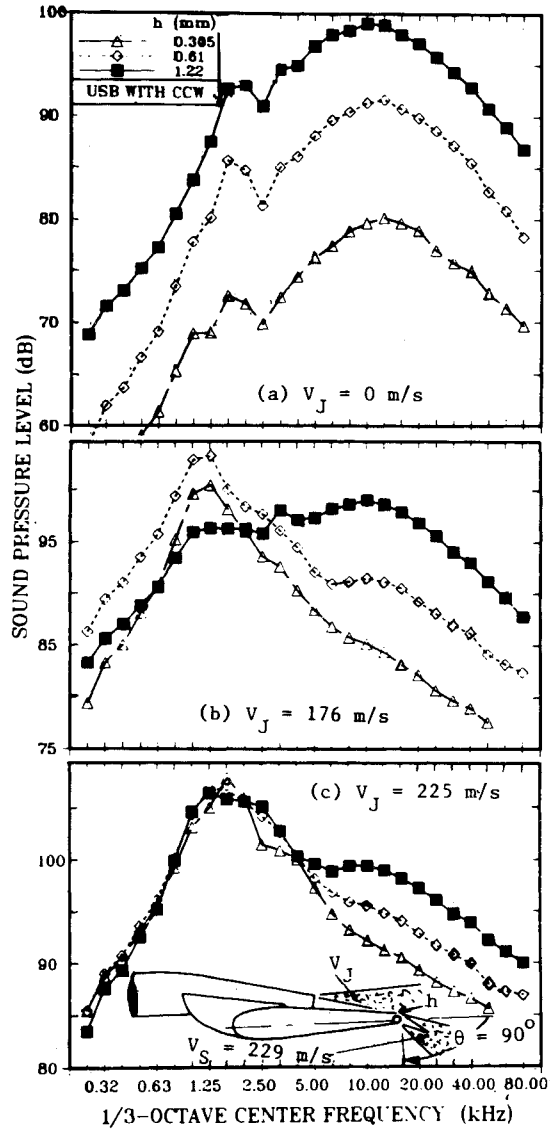

Fig. 19 Spectral variation with slot height h at various jet velocities, V_J; $\theta = 90$ deg; $V_T = 0$ m/s; $V_S = 229$ m/s.

Spectra

Typical ⅓-octave spectra at various polar angles are shown in Fig. 15. The most common thread of all these results is that, similar to jet mixing noise from round jets, the peak noise occurs at small angles to the jet axis.

Jet Velocity Dependence

The effect of V_J is examined by plotting the SPL spectra for different V_J at a number of slot velocities with $h = 1.22$ mm in Fig. 16. In this figure, the high frequency noise levels increase with increasing slot velocity. At $V_S = 0$ m/s, the effect of V_J is to increase the spectral level throughout the frequency range. However, as the CCW jet is turned on, the high frequency noise is increased much more significantly than it is by increasing V_J.

How the USB/CCW noise varies with jet velocity for different slot heights is shown in Fig. 17. The effects of changing V_S or h are basically the same, since the slot-jet momentum is altered by changing V_S or h. The only other effect observed in Fig. 17 is that the effect of V_J is to increase the SPL's even in the higher frequency range for smaller slot heights. This is because the slot jet momentum at lower slot

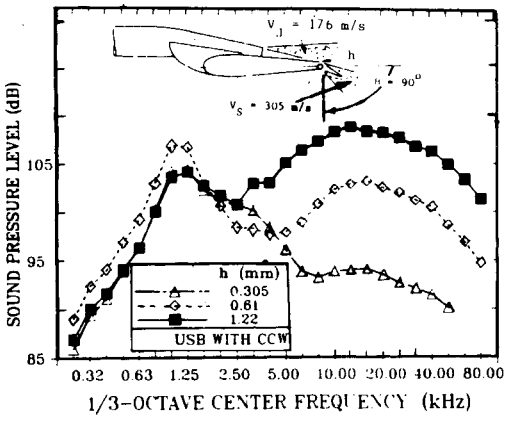

Fig. 20 Spectral variation with slot height h; $V_S = 305$ m/s; $\theta = 90$ deg; $V_T = 0$ m/s; $V_J = 176$ m/s.

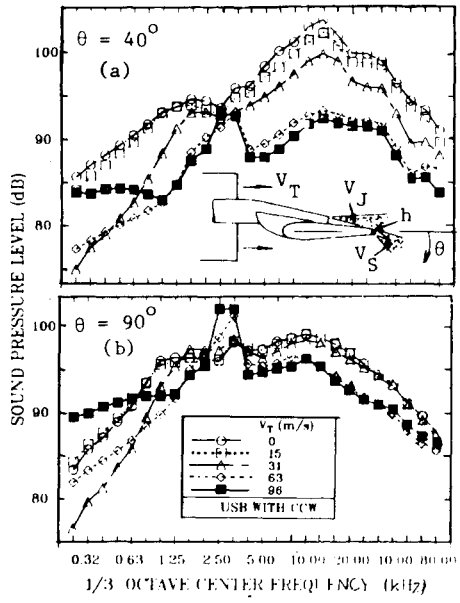

Fig. 21 Spectral variation with flight velocity V_T at two emission angles θ; $V_J = 176$ m/s; $V_S = 229$ m/s; $h = 1.22$ mm.

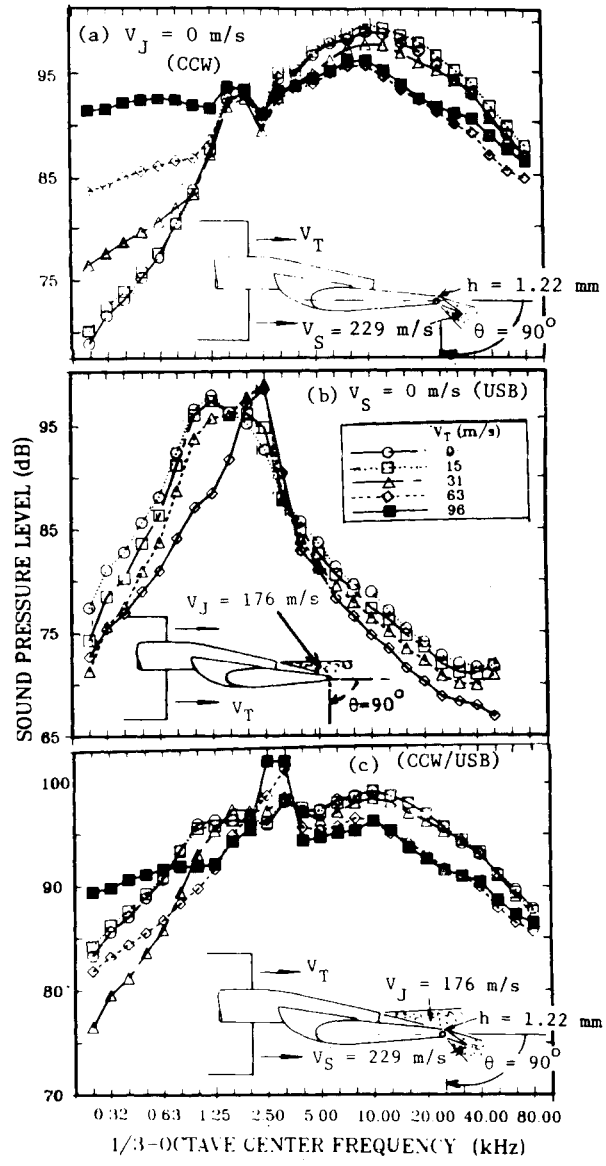

Fig. 22 Spectral variation with flight velocity V_T; $\theta = 90$ deg; $h = 1.22$ mm.

heights is too small to generate enough noise to dominate the USB jet noise.

In summary, therefore, at all angles the effect of USB jet velocity is felt at low frequencies for all slot velocities and frequencies for low slot velocities.

Slot Velocity Dependence

To examine the effect of increasing slot velocity on CCW/USB noise, the SPL's are plotted as a function of slot velocity at two jet velocities in Fig. 18. The sound pressure levels at all frequencies and the peak SPL frequency increase with increasing slot velocity.

Slot Height Dependence

In Fig. 19, the SPL spectra for different jet velocities at $\theta = 90$ deg are shown as a function of slot height h. As observed in the CCW-alone case, the SPL levels increase throughout the frequency range with increasing V_S. However, in the presence of USB flow, the low frequency noise does not depend much on slot height. In addition, the low frequency peak level becomes dominant over the high frequency peak with increasing V_J.

The effect of slot height is examined on the basis of different slot velocities in Fig. 20. Clearly, the high frequency noise increases with increasing h. It was found that the dominance of the high frequency noise is increased with increasing V_S.

Flight Velocity Dependence

Typical effects of free-jet velocity on the SPL spectra at two emission angles are shown for fixed V_J, V_S, and h in Fig. 21. The results indicated, in general, that flight simulation reduces noise at all angles at frequencies above 3–4 kHz. At lower frequencies, no set trend is observed. The sources of this behavior are traceable to similar results obtained for the CCW-alone and USB-alone configurations. For the CCW case (see Fig. 22a), flight simulation reduces the high frequency noise, but increases the low frequency noise. However, for the USB case, as shown in Fig. 22b, both low and high frequency noise levels decrease with flight. Since the low frequency noise is somewhat equally and oppositely modified by the USB and the CC effects, the combined SPL's for the CCW/USB do not show any particular trend, as shown in Fig. 22c. The above tendency was observed for various USB and slot velocities.[9]

The effect of free-jet velocity on the CCW/USB noise levels is examined at different slot heights for a fixed V_J and

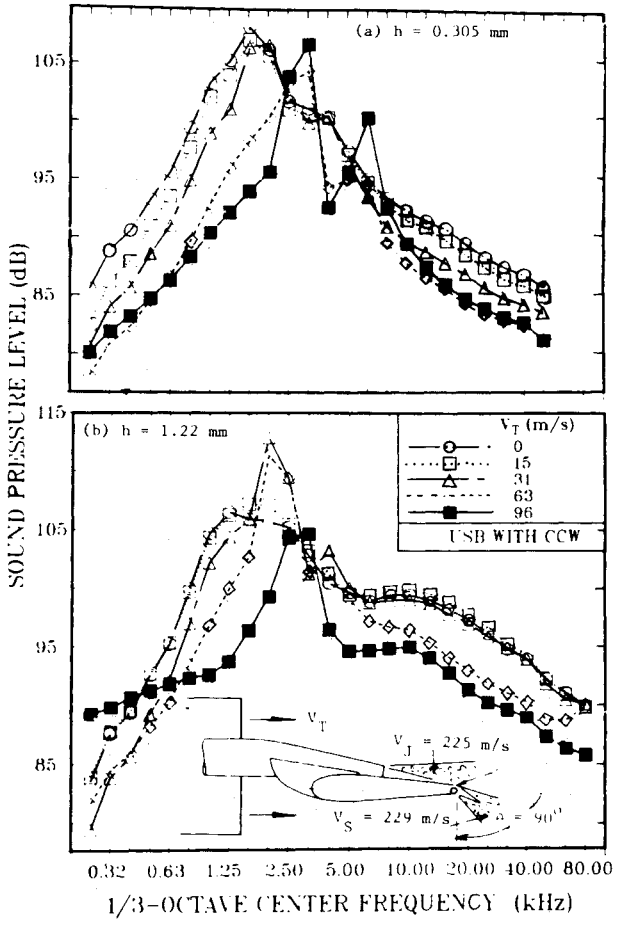

Fig. 23 Spectral variation with flight velocity V_T at two slot heights h; $\theta = 90$ deg; $V_J = 225$ m/s; $V_S = 229$ m/s.

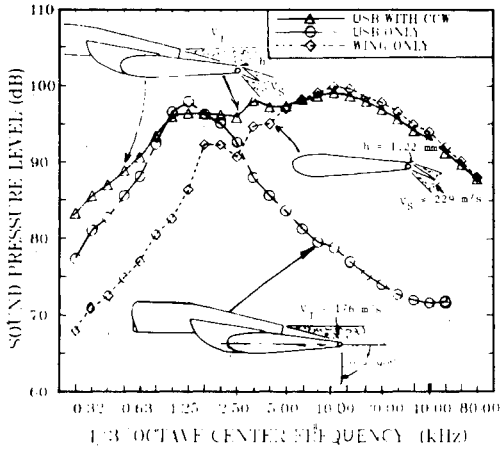

Fig. 24 Spectral data for different configurations; $\theta = 90$ deg; $V_T = 0$ m/s; $V_J = 176$ m/s; $V_S = 229$ m/s; $h = 1.22$ mm.

V_S in Fig. 23. At $h = 0.305$ mm, where the SPL's are dominated by V_J, the noise levels reduce with V_T at low and very high frequency regions; in the mid-frequency range, there is no clear trend. With increased slot height, the slot momentum is increased enough to contribute to the SPL's over the complete frequency range. Now, the trend in the low frequency range is driven by two opposing effects due to the CCW and the USB effects. However, the increase in high frequency SPL's due to higher slot-jet momentum made the frequency range wider, over which a reduction in SPL's with increasing V_T is observed.

Conclusion

Spectral distributions of sound pressure levels for the CCW/USB system and its components for a typical flow condition are summarized in Fig. 24. The spectral distribution of SPL's for the CCW/USB system has two parts; the dominant low frequency component is produced by the upper surface blowing, whereas the dominant high frequency component is due to the circulation control jet. Therefore, a possible way to predict the noise characteristics of the CCW/USB system is to formulate two separate prediction schemes which are based on the noise characteristics of the circulation control and the upper surface blowing. Similarly, the scaling parameter of the CCW/USB noise characteristics should be separated into two frequency regions; one for the low frequency and the other for the high frequency.

All the experimental results of this test program can be extrapolated to a full scale aircraft CCW/USB system by using proper scaling parameters. The present CCW/USB model is, basically, a 1/8th to 1/10th scale representation of a reasonably standard full scale aircraft wing-nozzle system. On this basis, all the frequencies should be scaled down by 8 or 10. The low frequency SPL peak (due to the USB), which appears around 1.25 kHz, will have a frequency of 120 to 140 Hz for a full scale aircraft.

The high frequency noise due to the circulation control should follow the same logic. However, in the present model the slot is much bigger than that of a proportionately scaled model; this is due to the limitations imposed by the instrumentation. The slot height used for the present model, for example, $h = 1.22$ mm, is even larger than some full scale circulation control slots might be. Therefore, the scaling in this case would increase the frequency. For example, the high frequency SPL peak appearing here at about 12.5 kHz would appear in the 20 to 25 kHz range for a full scale aircraft. This scaling, therefore, shifts this noise to a nonaudible frequency range. Since in most of the operating conditions the high frequency noise is dominant for the USB/CCW system, this noise will not cause any community annoyance problem. Therefore, the aerodynamic advantages of this high lift system can be successfully utilized without causing any significant noise problem.

Acknowledgments

This work was supported by Lockheed's Independent Research and Development Program. The authors are grateful to Dr. H. K. Tanna for initiating and planning the test matrix for this project. The contributions of Dr. J. Lepicovsky and Messrs. R. H. Burrin, D. E. Lilley, C. Leone, and J. F. Songer during various stages of design, data acquisition, and analysis are particularly acknowledged.

References

[1]Englar, R. J., Stone, M. B., and Hall, M., "Circulation Control—An Updated Bibliography of DTNSRDC Research and Selected Outside References," DTNSRDC Rept. 77-076, 1977.

[2]Englar, R. J., Trobaugh, L. A., and Hemmerly, R. A., "STOL Potential of the Circulation Control Wing for High-Performance Aircraft," *Journal of Aircraft*, Vol. 15, March 1978, pp. 175-181.

[3]Englar, R. J., "Investigation into and Application of the High Velocity Circulation Control Wall Jet for High Lift and Drag Generation on STOL Aircraft," AIAA Paper 74-502, 1974.

[4]Englar, R. J., "Subsonic Two-Dimensional Wind Tunnel Investigations of the High Lift Capability of Circulation Control Wing Sections," Naval Ship Research and Development Center Rept. ASED-274, 1975.

[5]Riebe, J. M., "A Correlation of Two-Dimensional Data on Lift Coefficient Available with Blowing-, Suction-, Slotted-, and Plain-Flap High Lift Devices," NACA RM L55D29a, 1955.

[6]Sleeman, W. C. and Hohlweg, W. C., "Low-Speed Wind-Tunnel Investigation of a Four-Engine Upper Surface Blowing Model Having a Swept Wing and Rectangular and D-shaped Exhaust Nozzles," NASA TN D-8061, 1975.

[7]Englar, R. J., "Development of the A-6/Circulation Control Wing Flight Demonstrator Configuration," DTNSRDC Rept. ASED-79/01, 1979.
[8]Nichols, J. H. Jr. and Englar, R. J., "Advanced Circulation Control Wing System for Navy STOL Aircraft," AIAA Paper 80-1825, 1980.
[9]Salikuddin, M., Brown, W. H., and Ahuja, K. K., "Noise from Circulation Control Wing with Upper Surface Blowing—Vol. I, Detailed Results," LG84ER0129, Lockheed-Georgia Co., Marietta, GA, 1984.
[10]Brown, W. H., Salikuddin, M., and Ahuja, K. K., "Noise from Circulation Control Wing with Upper Surface Blowing—Vol. II, Summary," LG84ER0130, Lockheed-Georgia Co., Marietta, GA, 1984.
[11]Salikuddin, M., and Brown, W. H., "Noise from Circulation Control Wing with Upper Surface Blowing—Vol. III, Tabulated Data," LG84ER0164, Lockheed-Georgia Co., Marietta, GA, 1984.
[12]Ahuja, K. K., Tester, B. J., and Tanna, H. K., "The Free Jet as a Simulator of Forward Velocity Effects on Jet Noise," NASA CR-3056, 1978.
[13]Englar, R. J., Nichols, J. H. Jr., Harris, M. J., and Huson, G., "Experimental Development of an Advanced Circulation Control Wing System for Navy STOL Aircraft," AIAA Paper 81-0151, 1981.
[14]Eppel, J. C., Shovlin, M. D., Jaynes, D. N., Englar, R. J., and Nichols, J. H. Jr., "Static Investigation of the Circulation-Control-Wing/Upper-Surface-Blowing Concept Applied to the Quiet Short-Haul Research Aircraft," NASA TM-84232, 1982.